THE JOURNAL OF BIOLOGICAL CHEMISTRY VOL. 290, NO. 28, pp. 17339–17348, July 10, 2015

Diversity in Overall Activity Regulation of Ribonucleotide Reductase*

Received for publication, March 5, 2015, and in revised form, May 12, 2015 Published, JBC Papers in Press, May 13, 2015, DOI 10.1074/jbc.M115.649624

Venkateswara Rao Jonna[‡], Mikael Crona[§1], Reza Rofougaran[‡1], Daniel Lundin[§], Samuel Johansson[‡], Kristoffer Brännström[‡], Britt-Marie Sjöberg[§], and Anders Hofer[‡2]

From the [‡]Department of Medical Biochemistry and Biophysics, Umeå University, SE-901 87 Umeå and the [§]Department of Biochemistry and Biophysics, Stockholm University, SE-106 91 Stockholm, Sweden

Background: Ribonucleotide reductase (RNR) makes DNA building blocks.
Results: Binding of three dATP molecules to the *Pseudomonas aeruginosa* class I RNR α subunit inactivates the enzyme by inducing an inert α_4 complex.
Conclusion: The number of bound dATP molecules and the tetrameric complex are unique among RNRs.
Significance: The novel inhibition mechanism of *P. aeruginosa* RNR is a potential drug target.

Ribonucleotide reductase (RNR) catalyzes the reduction of ribonucleotides to the corresponding deoxyribonucleotides, which are used as building blocks for DNA replication and repair. This process is tightly regulated via two allosteric sites, the specificity site (s-site) and the overall activity site (a-site). The a-site resides in an N-terminal ATP cone domain that binds dATP or ATP and functions as an on/off switch, whereas the composite s-site binds ATP, dATP, dTTP, or dGTP and determines which substrate to reduce. There are three classes of RNRs, and class I RNRs consist of different combinations of α and β subunits. In eukaryotic and *Escherichia coli* class I RNRs, dATP inhibits enzyme activity through the formation of inactive α_6 and $\alpha_4\beta_4$ complexes, respectively. Here we show that the *Pseudomonas aeruginosa* class I RNR has a duplicated ATP cone domain and represents a third mechanism of overall activity regulation. Each α polypeptide binds three dATP molecules, and the N-terminal ATP cone is critical for binding two of the dATPs because a truncated protein lacking this cone could only bind dATP to its s-site. ATP activates the enzyme solely by preventing dATP from binding. The dATP-induced inactive form is an α_4 complex, which can interact with β_2 to form a non-productive $\alpha_4\beta_2$ complex. Other allosteric effectors induce a mixture of α_2 and α_4 forms, with the former being able to interact with β_2 to form active $\alpha_2\beta_2$ complexes. The unique features of the *P. aeruginosa* RNR are interesting both from evolutionary and drug discovery perspectives.

Ribonucleotide reductase (RNR)[3] catalyzes the rate-limiting step in the only known *de novo* pathway for synthesis of DNA building blocks by reducing ribonucleoside di- or triphosphates (NDPs or NTPs) to the corresponding deoxyribonucleoside di- or triphosphates (dNDPs or dNTPs). High requirements for dNTPs in cancer cells and proliferating pathogens together with the lack of alternative pathways make RNR an interesting therapeutic target. RNRs are divided into three classes sharing a common fold but differing in how they generate the free radical that is essential for catalysis (1–3). Class I RNR enzymes, the dominating class in eukaryotes, common in bacteria, and also found in some archaea and double-stranded DNA viruses, consist of a catalytic protein, R1 (or α_2), and a smaller free radical-generating protein, R2 (or β_2). The minimal active form is an $\alpha_2\beta_2$ complex, but larger oligomeric complexes can also be formed (1). In contrast, class II RNR enzymes have only one subunit, and the free radical is generated from adenosylcobalamin. Class III RNR enzymes are anaerobic and use a dedicated activase to generate a stable glycine radical in the catalytic subunit. Based on the amino acid sequences of their catalytic subunits, the class I, II, and III RNRs are further divided into several NrdA/E, NrdJ, and NrdD subclasses.

Sophisticated allosteric regulation of RNR controls both the absolute concentrations of dNTPs in cells and the relative ratios of the four different dNTPs (1). Both of these controls are important for replication fidelity and DNA repair, and unbalanced dNTP pools are mutagenic (4). The two allosteric controls are implemented separately in the enzyme (1). Ratios between different dNTPs are controlled by substrate specificity regulation that occurs by binding of effector nucleotides to the specificity site (s-site) in the catalytic subunit. In class I enzymes that use NDPs as substrates, the binding of dATP/ATP induces CDP/UDP reduction, whereas dTTP and dGTP binding induce GDP and ADP reduction, respectively. The s-site and how it affects the active site to control substrate specificity is conserved in all three RNR classes. In contrast, the control of the absolute dNTP concentration by overall activity regulation of RNR is more unevenly distributed. This regulation has been found only in RNRs with an N-terminal ATP cone (5), which makes up the overall activity site (a-site).

Overall activity is regulated by competitive binding of ATP or dATP to the a-site (1). When levels of dNTPs are low, the ATP

* This work was supported by grants form the Kempe Foundation (to A. H.), Carl Trygger's Foundation (to A. H. and B. M. S.), the Swedish Cancer Foundation (to B. M. S.), the Swedish Research Council (to A. H. and B. M. S.), and the Wenner-Gren Foundations (to B. M. S.). The authors declare that they have no conflicts of interest with the contents of this article.
[1] Both authors contributed equally to this work.
[2] To whom correspondence should be addressed. Tel.: 46-70-2974096; E-mail: anders.hofer@medchem.umu.se.
[3] The abbreviations used are: RNR, ribonucleotide reductase; NDPs, nucleoside diphosphates; s-site, specificity site; a-site, overall activity site; GEMMA, gas-phase electrophoretic mobility macromolecule analysis.

cone will preferentially bind ATP and the enzyme is active. Conversely, when dNTP levels are sufficiently high, dATP will bind the a-site and inhibit enzyme activity. Mechanistically, the process has been primarily studied in enzymes from two class I RNR subclasses, NrdAg from *Escherichia coli* and NrdAe from humans, mice, *Saccharomyces cerevisiae* (RNR1), and the slime mold *Dictyostelium discoideum* (6–13). There are similarities, but also clear differences, in action between the bacterial *E. coli* RNR and the eukaryotic enzymes. In both mechanisms, high dNTP levels mediate oligomerization into tight complexes of larger size than the common $\alpha_2\beta_2$ complex, and the β_2 and α_{2n} subunits can no longer interact in a productive way. In the eukaryotic class I enzymes, the overall activity regulation relies on two different types of α_6 complexes depending on whether dATP or ATP binds to the a-site (8, 9). The dATP-inhibited complex binds the β_2 subunit in the center of the α_6 ring in such a way that the electron transport chain between the β and α subunits is disrupted. Less is known about the ATP-induced α_6 complex, which has not been crystallized, but mutagenesis studies have indicated that it is structurally different from the inactive complex (9) and gel filtration analysis shows that it might bind up to three β_2 subunits (12).

The corresponding class I enzyme from *E. coli* uses another mechanism of overall activity regulation. In this case, the enzyme activity is turned off via dimerization of the active $\alpha_2\beta_2$ form into an inactive ring-shaped $\alpha_4\beta_4$ complex that cannot support electron transport between the subunits (6, 7, 13). Thus in *E. coli* both subunits are needed for oligomerization, whereas the eukaryotic α subunit can form hexamers on its own. Furthermore, the *E. coli* enzyme can be inhibited by dATP as well as by combinations of ATP and high concentrations of dTTP or dGTP (7). The overall activity regulation of the *E. coli* enzyme thus appears to be governed by cross-talk between the a-site and s-site, whereas the overall activity regulation of the eukaryotic enzyme seems to be entirely driven by the a-site.

The different overall activity mechanisms found in eukaryotes and *E. coli* raises the question of whether the picture we have today of one eukaryotic and one bacterial mechanism is complete or if there are additional mechanisms to be discovered. More mechanisms can possibly be anticipated based on the extensive subclassification of RNRs and the distribution of ATP cones among them. The ATP cone is not found in all RNRs, suggesting that it has been gained and lost occasionally during evolution. Independent gains of an ATP cone could possibly lead to mechanistic differences in activity regulation. A particularly interesting example of an ATP cone gain is found in the class I RNR from *Pseudomonas aeruginosa* (NrdAz), which has two consecutive ATP cones. Earlier mutagenesis studies have indicated that only the first ATP cone has a role in overall activity regulation because its removal (the NrdA-Δ147 mutant) abolishes dATP inhibition and the ability to oligomerize in the presence of ATP (14). The second ATP cone seems to be needed for core functions because the removal of both cones leads to complete loss of enzyme activity (14). An additional ATP cone between the N-terminal ATP cone and the core of the protein might have implications for which inhibited complexes can be formed. In the previous analysis of the *P. aeruginosa* class I RNR, the size determination of the ATP-induced oligomers was ambiguous (14), which is a common problem with gel filtration analysis of protein complexes in rapid equilibrium. In this study we have used gas-phase electrophoretic mobility macromolecule analysis (GEMMA), which is an alternative method better suited for equilibrating complexes that has successfully been used for studies of other RNRs (7, 8, 10).

We show that RNRs with multiple ATP cones are much more common among RNRs than previously realized and that the *P. aeruginosa* class I RNR indeed differs in several aspects from both the eukaryotic and the *E. coli* mechanistic models of overall activity regulation. The *P. aeruginosa* enzyme is the first known example of an RNR that can bind three dATP per α polypeptide. Furthermore, the dATP-inhibited form in this case is an α_4 complex and ATP has a more passive role in the overall regulation than in the previously characterized models. The distinct differences in quaternary structures number of ATP cones among RNRs suggest that the mechanism of activity regulation might form the basis for the development of novel antibiotics.

Experimental Procedures

ATP Cone Counting—All sequences for each subclass in RNRdb2 release 0.9001 were downloaded from the NCBI (this functionality was still lacking from RNRdb2 when this work was performed). The ATP cone domain (PF03477) from the protein family database Pfam was used to search all unique sequences in RNRdb2 using the Hidden Markov Modeling-based software HMMER with its default settings. The identified domains in unique sequences were counted.

Purification of P. aeruginosa RNR—The *P. aeruginosa* α (107.1 kDa), α-Δ147 (91.3 kDa), and β (47.4 kDa) subunits were expressed and purified as described previously (14). The specific activities of the α, α-Δ147, and β subunits (assayed with 0.3 μM polypeptide) were 123, 100, and 250 nmol $\times$ min^{-1} $\times$ mg^{-1}, respectively, as measured with 0.7 mM CDP as the substrate, 3 mM ATP as the allosteric effector, and the non-limiting subunit at 5.6 times molar excess.

Enzyme Assays and Filter Binding Experiments—Unless otherwise indicated, the RNR enzyme assays were performed with the α and β subunits at 0.3 and 0.6 μM, respectively, in a buffer containing 30 mM dithiothreitol (DTT), 10 μM $FeCl_3$, 30 mM magnesium acetate, 0.5 mM substrate, allosteric effectors (see figure legends), and 30 mM Tris-HCl (pH 7.6) at 25 °C for 20 min. The enzyme reaction was stopped by heating the sample to 100 °C for 2 min, and the products were separated from substrates by boronate chromatography. The products in the flow-through were either measured by scintillation counting (in the radioactivity assay) or by HPLC (in the four-substrate assay) (7). In the filter binding assays, which were performed at 4 °C as described previously (15), the α subunit was incubated with 2 mM DTT, 30 mM magnesium acetate, 50 mM Tris-HCl (pH 7.6), and radiolabeled and unlabeled nucleotides at concentrations indicated in the figure legends.

GEMMA—For GEMMA analysis, which was essentially performed as described previously (7), the α subunits and/or β subunits (at 0.4 μM unless otherwise stated) were incubated in a buffer containing 20 mM ammonium acetate, 0.005% Tween 20 (only for the α subunit), and nucleotides as indicated in the

figure legends. GEMMA analysis was performed at reduced pressure (1.4–2 psi) to minimize interference from nucleotides and Mg^{2+} on the size measurement. Each sample was scanned 3–5 times, and a density of 0.58 g/cm^3 was used for conversion from diameter to molecular mass.

Gel Filtration—To confirm the GEMMA data for the β subunit, gel filtration analysis was performed on a Superdex 200 column with a mobile phase containing 150 mM KCl and 50 mM Tris-HCl (pH 7.6) and a flow rate of 0.5 ml/min. The β subunit (30 μg) was loaded using a 100-μl injection volume. The molecular mass was determined by comparing the retention time to that of a standard consisting of myoglobin (16.9 kDa), ovalbumin (45 kDa), transferrin (78 kDa), IgG (150 kDa), ferritin (440 kDa), and thyroglobulin (670 kDa). The proteins were mixed with mobile phase before loading.

Isothermal Calorimetry—Binding experiments were performed using an Auto-iTC$_{200}$ (MicroCal, GE Healthcare) at 25 °C. Protein concentrations were 20 μM dATP-induced α_4 tetramer in the cell and 325 μM β_2 dimer in the syringe. For the control experiment, 325 μM β_2 dimer was titrated into the cell with buffer (0.5 mM dATP, 30 mM magnesium acetate, and 30 mM Tris-HCl (pH 7.6)). For each experiment, we performed 19 automated injections of 2 μl each (duration 0.8 s) with 300-s intervals between each injection and with a stirring speed of 1000 rpm. A small preinjection (the first 0.4 μl) was performed 1500 s prior to the main injection to reduce the background signal. The titrations were carried out with high feedback and a filter period of 5 s.

Results

P. aeruginosa Class I RNR Belongs to a Subclass with Varying Numbers of ATP Cones—A bioinformatics analysis was performed to determine how common multiple ATP cones are in RNRs. We first searched all unique RNR sequences found in the non-redundant database of NCBI with the Pfam ATP cone domain (PF03477) to determine the number of ATP cones in the three RNR classes as well as in the new subclasses proposed in RNRdb2 (Table 1). Confirming common wisdom in the field, ATP cones, and thus activity regulation, are rare in class II RNRs (7%), more common in class I (47%), and most common in class III sequences where the majority (76%) has at least one ATP cone. Class I RNRs lacking ATP cones are dominated by the NrdE subclass (identical to the traditional subclass Ib) containing more than one-third of the known class I sequences (37%), none of which have any identifiable ATP cones. Among the remaining class I RNRs, 78% have at least one ATP cone. Interestingly, multiple ATP cones are fairly common and are found in all RNR classes and many of the subclasses. They are especially common in the NrdAz subclass that includes the *P. aeruginosa* and the *Chlamydia trachomatis* class I RNRs, both of which are well known for carrying multiple ATP cones (14, 16).

The N-terminal ATP cone in the *P. aeruginosa* α subunit was found to be much more similar to the Pfam profile than the second ATP cone (Table 2) (17–32). In fact, all *Pseudomonas* spp. (only *P. aeruginosa* is shown in the table) have very similar scores for their two N-terminal ATP cones (average HMMER scores of 70.0 ± 4.5 and 27.9 ± 4.4). Amino acid sequence analysis showed important differences in the second ATP cone compared with the Pfam profile, with the most striking one being an Arg to Ala substitution in the highly conserved KR(D/N) motif (Fig. 1). The Arg residue is involved in the binding of the ATP/dATP phosphate moieties (9). The NrdAz subclass also includes *Chlamydia* and *Chlamydophila* species, which all have three ATP cones (only *C. trachomatis* is shown in Table 2). The first two ATP cones appear functional judging by their high similarities to the profile (average HMMER scores of 71.1 ± 10.7 and 66.0 ± 14.6). The N-terminal ATP cone in most NrdAz sequences is the one that is best preserved judging by its similarity to the profile (the N-terminal ATP cone has the highest HMMER score in 478 of 485 NrdAz sequences compared with only 7 for the second ATP cone and 0 for the third). Twenty-one NrdAz sequences have a second ATP cone that is almost as similar to the profile as the first, or in a few cases more similar, and thus appears to be functional.

TABLE 1
ATP cone distribution of different RNR classes and subclasses
The right column shows how many sequences the frequency is based on. The predominant number of ATP cones in each subclass is in bold.

Class	Subclass	Frequency of number of ATP cones (%)				Number of sequences
		0	1	2	3	
I (NrdA/E)		53	33	13	1	4186
I	NrdAe	9	**90**	1	0	630
I	NrdAg	4	**96**	0	0	688
I	NrdAh	37	**31**	32	0	326
I	NrdAi	**100**	0	0	0	122
I	NrdAk	**100**	0	0	0	158
I	NrdAn	**58**	37	4	0	89
I	NrdAz	10	3	**82**	5	541
I	NrdE	**100**	0	0	0	1532
II (NrdJ)		93	6	1	0.1	1800
II	NrdJd	**100**	0.4	0	0	541
II	NrdJf	**89**	9	2	0.1	1002
II	NrdJm	**95**	4	0.4	1	257
III (NrdD)		24	70	6	0.3	2426
III	NrdDa	18	36	**43**	3	74
III	NrdDb	33	**58**	9	0	457
III	NrdDc	13	**83**	4	0.2	1378
III	NrdDd	33	**64**	3	0	351
III	NrdDf	**100**	0	0	0	4
III	NrdDh	**69**	31	0	0	134
III	NrdDi	**100**	0	0	0	28

The P. aeruginosa α Subunit Can Bind Up to Three dATP Molecules per Polypeptide—All allosterically regulated RNRs characterized so far can bind either one or two dATP molecules to each α polypeptide (1), one in the s-site and for those that have an ATP cone, a second one in the a-site. To our surprise, a Scatchard plot from the filter binding assay with radiolabeled dATP showed that the *P. aeruginosa* α subunit could bind approximately three dATP molecules per polypeptide (n = 2.62 ± 0.06; K_D = 1.51 ± 0.10 μM) (Fig. 2*A*). This analysis, which is strongly dependent on the fraction of active protein, showed a significantly higher n value than reported before (14). All three allosteric sites seemed to have similar affinities, which is also a difference from other characterized RNRs where the s-site generally has much higher dATP affinity than the a-site.

Further characterization of the dATP binding sites showed that dTTP could compete out one of the three dATP molecules, whereas dGTP and ATP seemed to be able to compete out considerably more of the dATP (Fig. 2*B*). In one experimental series (*open squares* in Fig. 2*B*) where a constant high concen-

TABLE 2

Pfam profile HMMER score similarity of ATP cones in RNRs

The table shows the number of ATP cones and their HMMER scores as well as data (with indicated references) on dATP binding, dATP inhibition, and if any quaternary structure is associated with dATP inhibition. Inhibited complexes that can bind β_2 but are not dependent on it for their formation are written in their α form (e.g. α_4 rather than $\alpha_4\beta_2$ for *P. aeruginosa*). Included in the list are all RNRs known to have an ATP cone that binds dATP/ATP and a few additional RNRs of relevance.

Class	Subclass	Species	No of ATP cones	HMMER scores	dATP		Ref.
					Binding	Inhibition	
I	NrdAe	*D. discoideum*	1	63.1	Yes	Yes, α_6	10
I	NrdAe	*Mammalia*	1	65.0	Yes	Yes, α_6	9, 12, 17–20
I	NrdAe	*S. cerevisiae* RNR1	1	56.9	Yes[a]	Yes, α_6	9, 21
I	NrdAe	*S. cerevisiae* RNR3	1	55.3	ND[b]	No	21
I	NrdAe	*Trypanosoma brucei*	1	41.7	Yes	No	22, 23
I	NrdAe	Vaccinia virus	1	62.9	Yes[a]	Yes	24
I	NrdAg	Bacteriophage T4	1	64.6	Yes	No	25–27
I	NrdAg	*E. coli*	1	54.2	Yes	Yes, $\alpha_4\beta_4$	6, 7, 13, 28
I	NrdAz	*P. aeruginosa*	2	70.6; 31.8	Yes	Yes, α_4	14, this study
I	NrdAz	*C. trachomatis*	3	73.1; 68.3; 12.0	Yes[a]	Yes	16
II	NrdJf	*Pyrococcus furiosus*	1	79.4	Yes (?)[a]	Yes (?)[a]	29
II	NrdJf	*Thermoplasma acidophilum*	1	90.9	Yes	No	30
III	NrdDc	*E. coli*	1	73.0	Yes[c]		31
III	NrdDc	*Lactococcus lactis*	1	74.7	Yes[c]		32
III	NrdDd	*P. aeruginosa*	1	82.2	ND		

[a] Binding experiments have not been performed, but enzymatic data show that they have general dATP inhibition. The RNR from *P. furiosus* is marked with a question mark because the data behind the conclusion were not shown in the reference.
[b] ND, not determined.
[c] The effect of dATP is dependent on which nucleotide is occupying the s-site.

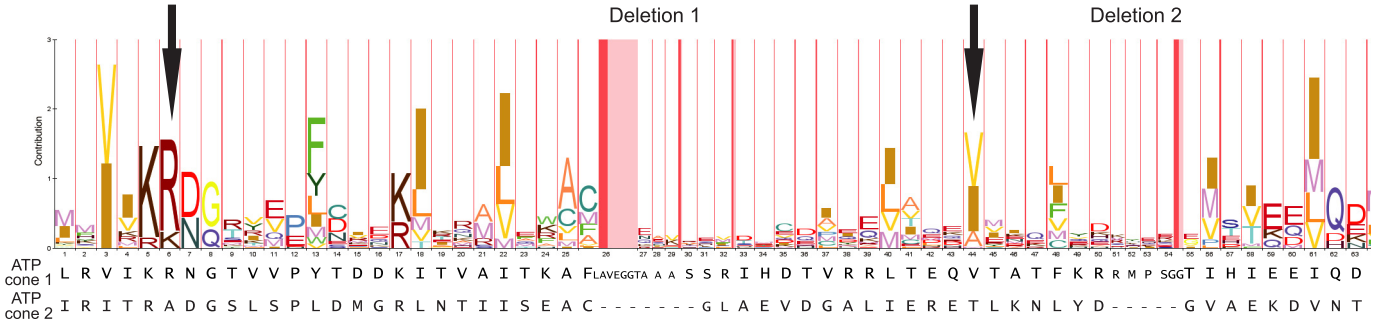

FIGURE 1. **Amino acid sequence alignment of the two ATP cones of the *P. aeruginosa* α subunit against the Pfam profile consensus sequence.** Important differences in the second ATP cone from the Pfam profile are highlighted, including an Arg to Ala substitution in the KR(D/N) motif, two deletions, and a hydrophobic residue substituted for a Thr. Only the first 63 of the 90 amino acids of the Pfam ATP cone are shown.

tration of unlabeled dTTP was present (4 mM) to prevent the binding of one of the three dATP molecules, an increasing concentration of unlabeled ATP was shown to compete out dATP from the two remaining sites.

A Scatchard plot of dGTP binding to the *P. aeruginosa* α subunit showed that the nucleotide was bound to one site with high affinity as indicated by the straight line in the beginning of the curve and that it was bound to the remaining sites with much lower affinity (Fig. 2*C*). Assuming one high affinity site and two low affinity sites, K_D values could be calculated as 1.15 ± 0.22 and 97 ± 9 μM, respectively. In a competition experiment using labeled dGTP at a concentration (80 μM) high enough to saturate the high affinity site and partially fill up the low affinity sites, dTTP could compete out one dGTP molecule, whereas dATP competed out all label (Fig. 2*D*). ATP could only compete out a minor fraction of the dGTP, which was consistent with the experiment in Fig. 2*B* (compare *open* and *filled squares*) where ATP was primarily competing for the type of sites where dTTP was not able to bind. We interpret these results as one typical s-site binding dGTP, dTTP, and dATP (and perhaps ATP) plus two a-sites binding dATP, ATP, and to some extent dGTP. The lower affinity of ATP than dNTPs for the s-site is typical for all studied RNRs and reflects the much higher concentration of ATP in the cell (1).

To better understand the nature of the two a-sites, binding experiments with the α-Δ147 subunit, which lacks the N-terminal ATP cone, were performed. The mutant subunit had only one dATP binding site (n = 1.16 ± 0.05; K_D = 2.29 ± 0.27 μM), which was concluded to be an s-site because the dATP was readily competed out with dTTP (Fig. 2, *E* and *F*). Removal of the first of the two ATP cones in the *P. aeruginosa* α subunit will, therefore, lead to loss of both a-site dATP molecules.

P. aeruginosa β *Subunit Is Predominantly a Dimer, whereas the* α *Subunit Is in a Nucleotide-dependent Equilibrium between Monomers, Dimers, and Tetramers*—GEMMA analysis of the β subunit showed that it is predominantly a dimer, although small amounts of monomers were also observed (Fig. 3*A*). We also performed gel filtration analysis of the protein (Fig. 4). Although the position of the main peak indicated a larger size than the 94-kDa dimer (calculated as 127 kDa from a standard curve based on the retention times of the standard globular proteins), it was still not large enough to indicate a tetrameric quaternary structure, which was what had been concluded in the earlier *P. aeruginosa* RNR study (14). The observed deviation between GEMMA and gel filtration could instead be due to that the protein is not entirely globular. Altogether, our GEMMA and gel filtration data indicate that the

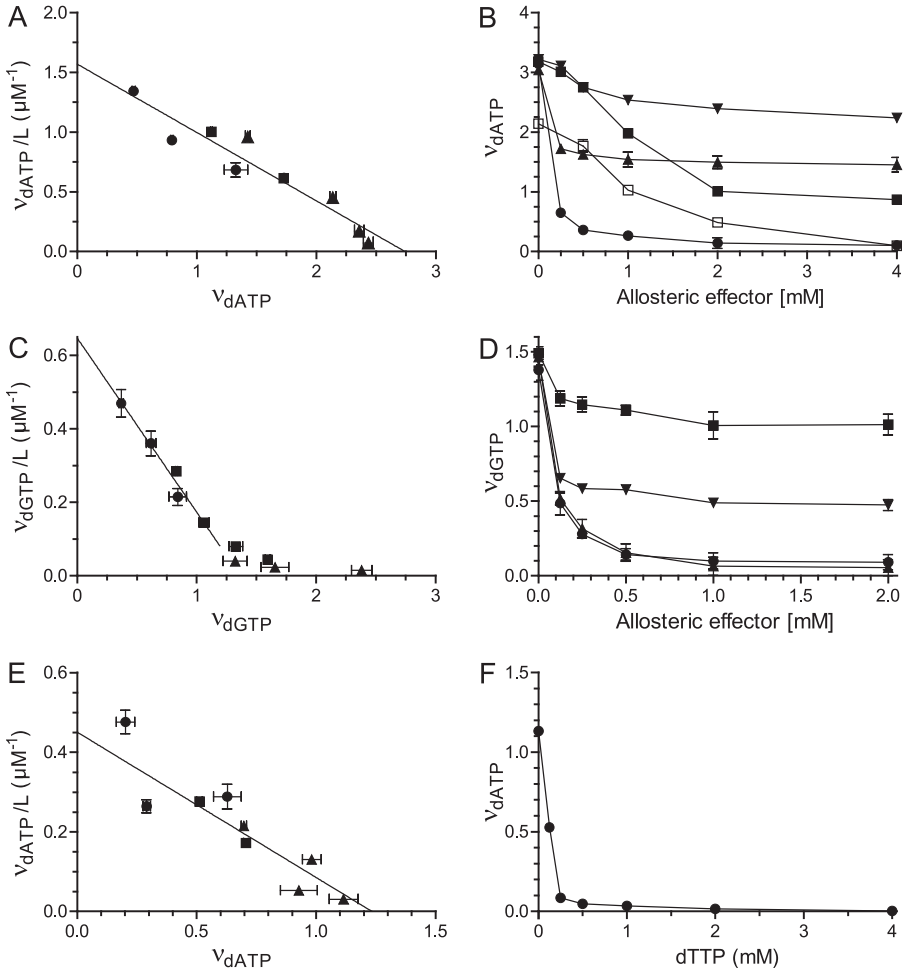

FIGURE 2. **Nucleotide binding experiments.** *A,* Scatchard plot showing the number of dATP binding sites in the α subunit. Experiments were performed with 0.5 μM (●), 1.25 μM (■), and 2.5 μM (▲) α subunit in *panels A* and *E*. *B,* competition experiments where 60 μM [^{3}H]dATP is competing with varying concentrations of unlabeled dTTP (▼), dGTP (▲), ATP (■), dATP (●), or a combination of ATP with 4 mM dTTP (□) for binding to 5 μM α protein. *C,* Scatchard plot showing the binding of dGTP to 1.25 (●), 2.5 (■), and 5 μM (▲) α subunit. *D,* competition experiments where 80 μM [^{3}H]dGTP is competing with varying concentrations of unlabeled dTTP (▼), dGTP (▲), ATP (■), or dATP (●) for binding to 15 μM α subunit. *E,* Scatchard plot showing the binding of dATP to the α-Δ147 subunit. *F*, competition experiments where 30 μM [^{3}H]dATP is competing with varying concentrations of unlabeled dTTP for binding to 3 μM α-Δ147 subunit. All graphs are based on the data from three separate experiments with standard errors indicated. The linear regression lines for *panels A*, *C*, and *E* (based on the first four points in *C*) are for visual purposes only, and the calculations of binding constants and number of sites in the text are based on non-linear regression of corresponding bound *versus* free ligand graphs.

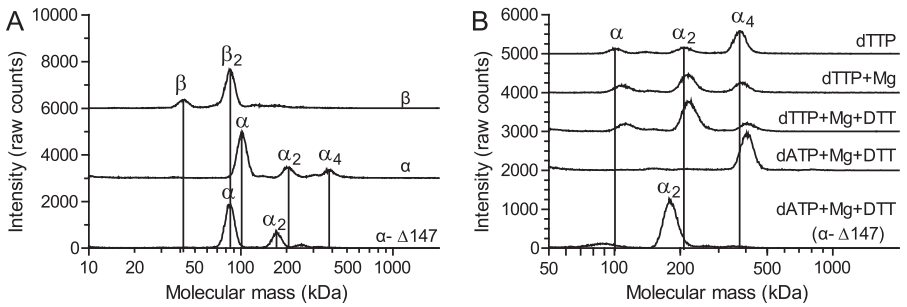

FIGURE 3. **GEMMA analysis of the *P. aeruginosa* β, α, and α-Δ147 subunits.** *A,* analysis of the three proteins in the absence of nucleotide effectors. The *lines centered below* the peaks indicate masses of 42 (β), 85 (β_2 and α-Δ147), 103 (α), 171 (α_2-Δ147), 201 (α_2), and 378 kDa (α_4). *B,* the distribution of α, α_2, and α_4 peaks in the presence of 50 μM dTTP (only equimolar Mg^{2+} was present), 50 μM dTTP + 1 mM Mg^{2+} (dTTP + Mg), 50 μM dTTP + 1 mM Mg^{2+} + 30 mM DTT (dTTP + Mg + DTT), or 50 μM dATP + 1 mM Mg^{2+} + 30 mM DTT (dATP + Mg + DTT). The *lines centered below* the peaks of the *upper trace* indicate molecular masses of 100 (α), 206 (α_2), and 376 kDa (α_4). The slight shift of the lower traces in *B* is due to nonspecific binding of Mg^{2+}. The assignments of the peaks in *A* and *B* were based on the theoretical masses of 107 (α), 91 (α-Δ147), and 47 kDa (β). The traces are spaced 3000 (*A*) and 1000 or 2000 (*B*) units apart to fit many experiments in the same graph.

P. aeruginosa β subunit quaternary structure does not differ from the dimeric form found in other species.

The α subunit was in a monomer-dimer-tetramer equilibrium (Fig. 3, *A* and *B*). The tetramer was not detected in the α-Δ147 mutant showing that this complex cannot be formed in the absence of the N-terminal a-site. In the wild-type α subunit, tetramer formation was strongly stimulated in the presence of allosteric effectors. Also dTTP, which only binds to the s-site,

was able to stimulate tetramer formation. However, in the presence of physiologically relevant Mg^{2+} concentrations (in the mM range), dimers dominated over tetramers, and this effect was even more pronounced in the presence of a reducing agent (DTT) that preserves the active form of the α subunit (Fig. 3*B*). In contrast, the dATP-induced tetramer was stable in the presence of Mg^{2+} and DTT. GEMMA is normally not very compatible with non-volatile chemicals, but because all experiments were performed at a reduced pressure to minimize the effect on the molecular mass of nonspecifically bound Mg^{2+} and nucleotides, the concentration of Mg^{2+} could be raised up to 1 mM with only a slight shift of the peak positions to the right. A conclusion from the experiments with the α subunit is that the a-site is an absolute requirement for tetramer formation and that the stability of the tetramer is affected by the nucleotide that is bound to it.

P. aeruginosa α_4 *and* $\alpha_4\beta_2$ *Complexes Predominate under Conditions in Which the Protein Is Inactive*—To determine which are the active and inactive forms of the *P. aeruginosa* RNR, a series of GEMMA experiments were undertaken where the enzyme was incubated with combinations of allosteric effectors and substrates (Fig. 5*A*). All experiments were performed in the presence of Mg^{2+} (1 mM) and reducing agent (30 mM DTT) to resemble the conditions when the enzyme is normally active. As seen in the top trace where both subunits were incubated with dTTP and GDP, two peaks appeared that were not observed when the α subunit was tested under similar conditions in the absence of the second subunit (*2nd trace*). One of the peaks is the free β_2 subunit, and the other has the molecular mass of an $\alpha_2\beta_2$ complex. In analogy with all characterized class I RNRs to date, this can be assumed to be an active form of the enzyme. In the remaining traces, the α protein was tested alone in the presence of different allosteric effector/substrate combinations. In all cases, there were dimer-tetramer equilibria, but in the presence of the activating allosteric effectors (dTTP and ATP) the equilibria were shifted toward dimers, and with the inhibiting allosteric effector (dATP) the equilibrium was shifted toward tetramers. Interestingly, dGTP, which has some a-site affinity (see Fig. 2), favored tetramers (Fig. 5*A*, *4th trace*). If the dGTP was combined with ATP, which only competes readily for the a-site (see Fig. 2*D*), the equilibrium shifted toward dimers (Fig. 5*A*, *5th trace*). The combination of dGTP in the s-site and ATP in the a-site thus seems to favor dimers. Tetramers induced by dATP were very stable as indicated by the fact that dimers were hardly visible (Fig. 5*A*, *bottom trace*).

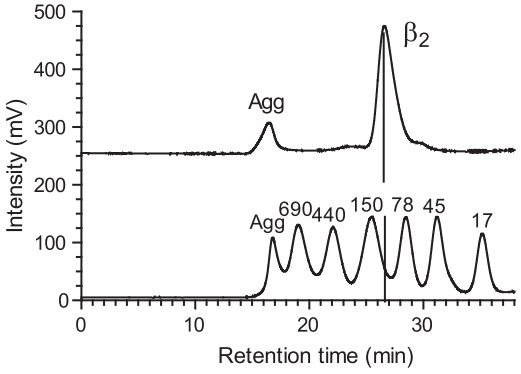

FIGURE 4. **Gel filtration analysis of the *P. aeruginosa* β subunit (*upper trace*) in comparison to a molecular mass standard of globular proteins (*lower trace*).** The masses of the standard proteins are indicated. The traces are spaced 250 units apart to fit both experiments in the same graph.

Fig. 5*B* shows the interaction between the dATP-induced α_4 complexes and the β subunit. These experiments were performed with 50 μM dATP concentrations with equimolar Mg^{2+} and without DTT to get more exact size measurements. The gradual addition of more β subunit led to a mass shift of ~65 kDa, which suggests that only one β_2 dimer binds to each α_4 tetramer. The shift remained the same even with higher concentrations of β subunit (data not shown). The $\alpha_4\beta_2$ structure was also supported by isothermal titration calorimetry where the β_2 dimer was titrated into a solution with dATP-induced α_4 tetramer (Fig. 6). The experiment was performed three times with similar results (Fig. 6 shows one of them). An average of the three experiments showed that one β_2 dimer ($n = 1.28 \pm 0.03$ S.E.) binds each α_4 tetramer, and this supports our conclusion that the inhibited form of the enzyme is an $\alpha_4\beta_2$ complex. The two subunits had a moderate affinity ($K_D = 2.28 \pm 0.05$ μM) for each other, and their interaction was primarily ΔH-driven ($\Delta H = -10.3 \pm 0.5$ kcal $\times$ mol^{-1}, $\Delta S = -8.6 \pm 1.8$ cal $\times$ mol^{-1} $\times$ K^{-1}). In this case, the solution contained 0.5 mM dATP and 30 mM magnesium acetate.

Role of a-site ATP in Enzyme Activity Regulation—A four-substrate assay showed that the *P. aeruginosa* class I RNR has similar specificity regulation as most other characterized RNRs (1), with ATP stimulating CDP reduction and dTTP and dGTP stimulating GDP and ADP reduction, respectively (Fig. 7*A*).

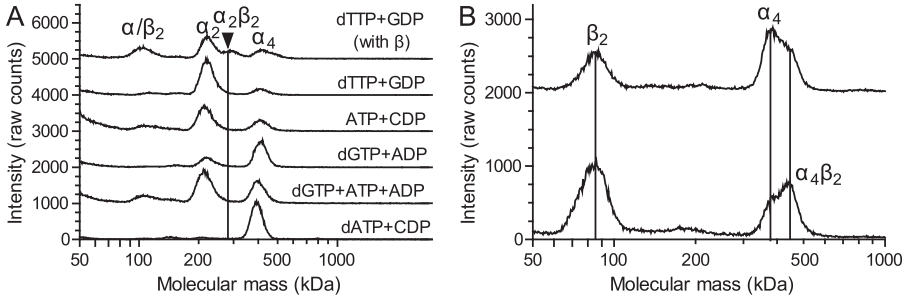

FIGURE 5. **GEMMA analysis of the α_4 complex to determine its nucleotide dependency (*A*) and interaction with the β subunit (*B*).** The proteins were incubated with 30 mM DTT and 1 mM magnesium acetate. The NDP substrate (100 μM) and allosteric effector (50 μM dNTP or 200 μM ATP) are indicated. The *vertical line* indicates the position of the $\alpha_2\beta_2$ complex, which was determined to be 286 kDa, whereas the positions of other peaks were similar as in Fig. 3*B*. *B*, the α subunit in the presence of dATP was incubated together with 1:1 and 1:2 molar ratios with the β subunit (*top* and *bottom traces*, respectively). The *lines* in *B* indicate masses of 85, 375, and 439 kDa. The traces are spaced 1000 (*A*) or 2000 (*B*) units apart to fit many experiments in the same graph.

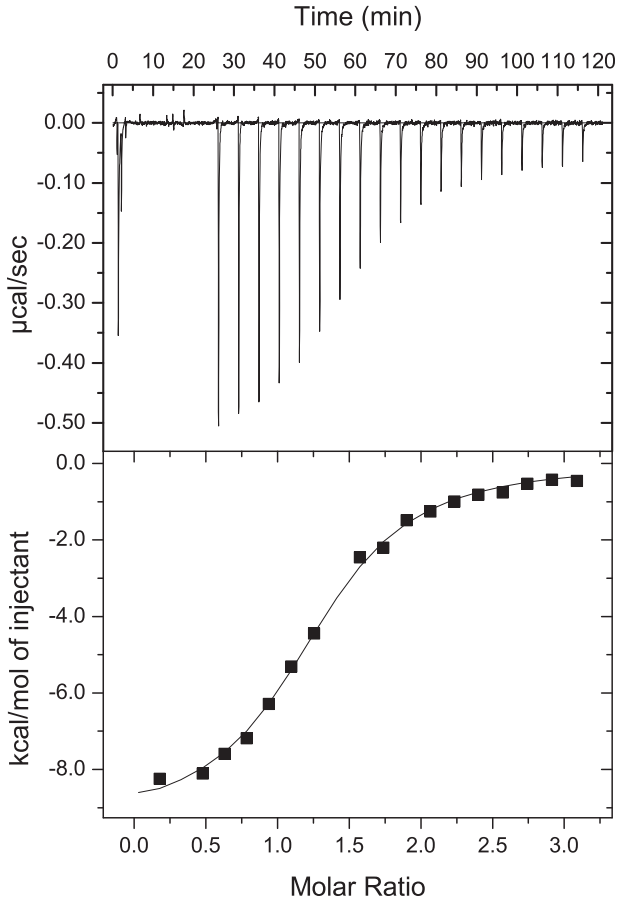

FIGURE 6. **Isothermal calorimetry analysis showing $\alpha_4\beta_2$ formation.** The β_2 dimer was titrated into a solution of dATP-induced α_4 tetramer. Both solutions contained 0.5 mM dATP and 30 mM magnesium acetate. Calorimetric data were plotted and fitted using the standard single-site binding model (Origin, MicroCal).

However, UDP seems to be a very poor substrate under all circumstances. To specifically study the effect of ATP binding to the a-site, experiments were also performed where ATP was combined with dGTP or dTTP at high enough concentrations to exclude ATP binding to the s-site (Fig. 7, *A–D*). As expected from its low affinity to the s-site, ATP addition did not affect the GDP and ADP specificity induced by 2 mM dTTP or dGTP, respectively (Fig. 7*A*). ATP instead increased the dGTP-induced ADP reduction. Because no such ATP effect was observed with dTTP-induced GDP reduction, we wanted to investigate whether this effect was related to the ability of dGTP to bind to the a-site. In Fig. 7*B*, the concentration of dGTP was reduced to 0.5 mM to decrease a-site occupancy. ATP did not have any obvious effect on dGTP-stimulated ADP reduction under these conditions, suggesting that the role of ATP is indirect, *i.e.* to compete out inhibitory dGTP from the a-site rather than having an effect on its own. The lack of direct ATP effects on enzyme activity via the a-site is illustrated in Fig. 7*C* where a comparison with the mouse enzyme was made. In the mouse RNR, the dTTP-promoted GDP reduction was strongly stimulated by ATP via the a-site, whereas it was not stimulated in the *P. aeruginosa* enzyme. The role of ATP as a passive regulator was further confirmed in Fig. 7*D*, where a higher concentration of dATP was needed to inhibit the enzyme in the presence of ATP than in its absence. The passive activation of ATP is ascribed to the a-site because any ATP binding to the s-site would lead to inhibition of GDP reduction rather than activation.

Discussion

Overall RNR activity regulation has until now been believed to occur by the binding of a single dATP molecule to the N-terminal ATP cone and thereby causing the formation of an inactive α_6 (eukaryotes) or $\alpha_4\beta_4$ (*E. coli*) complex. We now present a third model by showing that *P. aeruginosa* class I RNR binds

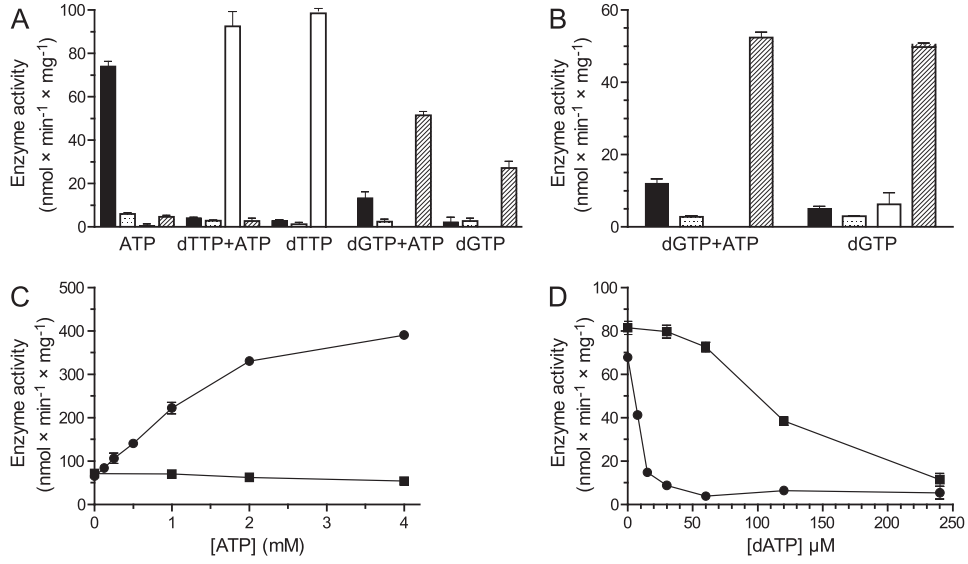

FIGURE 7. **Allosteric regulation of the *P. aeruginosa* class I RNR activity.** *A,* enzyme activity was measured with the indicated allosteric effectors (2 mM of each) and all four substrates present simultaneously (0.5 mM of each). The activities are shown with CDP (*solid bar*), UDP (*stippled*), GDP (*open*), and ADP (*hatched*). *B,* similar to the corresponding experiments in *A*, but the concentration of dGTP was only 0.5 mM. *C,* GDP reduction with the mouse (●) and *P. aeruginosa* (■) RNRs in the presence of 2 mM dTTP and increasing concentrations of ATP. *D,* GDP reduction with the *P. aeruginosa* RNR in the presence of 2 mM dTTP and increasing concentrations of dATP. The experiment was performed in the presence (■) and absence (●) of 3 mM ATP. Experiments were performed in triplicate (*A* and *B*) or duplicate (*C* and *D*) with the standard errors indicated.

two dATP molecules to its ATP cone and that the inactive complex is an α_4 tetramer.

The fact that regulation of RNR activity always involves an N-terminal ATP cone would perhaps suggest that it is an ancestral trait present in the common ancestor of modern RNRs. Speaking against this, however, is the patchy distribution of activity regulation and ATP cones among modern RNRs and that there is more than one mechanism to achieve overall activity regulation. We believe that evolution has repeatedly discovered the ATP cone as a way of regulating RNR activity, possibly aided by recombination between RNR genes. In this scenario, the ATP cone acts like a module that can be gained or lost depending on the requirement of the organism to exert control over the absolute concentration of dNTPs beyond transcriptional and other non-allosteric mechanisms. Supporting this scenario, we observed a much larger heterogeneity than expected in the distribution of RNR sequences with ATP cones, RNR sequences without ATP cones, and RNR sequences with multiple ATP cones among the different RNR classes and subclasses. In contrast, the substrate specificity regulation is much more conserved and common to all studied RNRs with the exception of *Herpesviridae* (33). It is, therefore, likely to represent the mechanism present in the ancestor of all modern RNRs. The regulation of *P. aeruginosa* RNR specificity is also similar to other species with the exception that UDP is a very poor substrate. It is therefore likely that *P. aeruginosa* gets most of its dTTP via CDP reduction followed by deamination rather than via UDP reduction. This alternative pathway is common in many species such as *E. coli* and mammalian cells (1).

A surprisingly large number of RNR sequences have multiple ATP cones. In most cases the second ATP cone appears nonfunctional, like in *P. aeruginosa*, but some, in particular the *Chlamydia* spp. and *Chlamydophila* spp. sequences, contain a second ATP cone with high HMMER scores indicating functionality (*C. trachomatis* is shown in Table 2). If the ATP cone and the activity regulation have been gained multiple times, details of the mechanism are expected to differ between RNRs because a recently gained ATP cone needs to adapt to the surrounding amino acid sequence to be able to form dATP-inhibited complexes. The different mechanisms identified in the eukaryotic, *E. coli*, and now *P. aeruginosa* RNRs support this hypothesis. Horizontal transfer of RNR genes and paralogy both in the form of multiple copies of proteins from the same class and encoding of several classes in the same genome are commonly found in organisms (34), and this provides a plausible scenario for how the ATP cone could have been transferred between different classes and subclasses of RNRs.

Common for the class I RNR family is that the α subunit can dimerize and interact with the β_2 subunit to form an active $\alpha_2\beta_2$ complex, although this tetramer is considered a minor form of the eukaryotic enzymes under physiological ATP concentrations (1). The α dimerization and the interaction between the two subunits are generally stimulated by allosteric effectors, whereas the a-site-binding effectors can also stimulate the formation of higher order complexes. To date, the overall activity regulation mechanism has only been studied in a few class I RNRs (1) representing three of the 10 subclasses, including NrdAe from mammals and other eukaryotes, NrdAg from

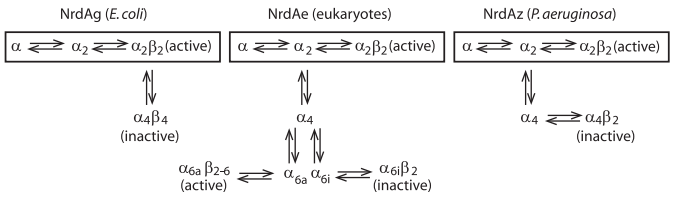

FIGURE 8. **Oligomerization of the *E. coli*, eukaryotic, and *P. aeruginosa* class I RNRs.** The *boxes* indicate general complexes in the class I RNR family. The eukaryotic hexamers are indicated with *a* and *i* to highlight active and inactive structural conformations, respectively. The eukaryotic α_4 complex is a hypothetical intermediate form.

E. coli, and, as reported here, NrdAz from *P. aeruginosa*. All have N-terminal ATP cones that appear functional based on their HMMER score (Table 2). As shown in Fig. 8, *P. aeruginosa* and eukaryotes have an α-driven oligomerization process in which two or three α_2 subunits associate to form a tetramer or a hexamer, respectively. In eukaryotes, ATP bound to the ATP cones of the α subunits opens the conformation of the hexamer to allow one, two, or three β_2 dimers to bind and form an active $\alpha_6\beta_{2-6}$ complex, whereas in *P. aeruginosa,* ATP (or empty a-sites) destabilizes the tetramer allowing the formation of α_2 and $\alpha_2\beta_2$ complexes. Although the active form in *E. coli* is the same $\alpha_2\beta_2$ complex as in *P. aeruginosa*, the equilibrium between active $\alpha_2\beta_2$ and inactive $\alpha_4\beta_4$ complexes requires interaction with the β subunit in *E. coli*. There are thus clear similarities between *P. aeruginosa* and eukaryotic class I RNRs in terms of how higher complexes are formed, but also similarities between the *P. aeruginosa* and *E. coli* class I enzymes in that the active form is an $\alpha_2\beta_2$ complex.

An interesting feature of the *P. aeruginosa* RNR is that although studies on the a-site mutant (α-Δ147) show that the a-site itself is a prerequisite for tetramer formation, it does not need to be occupied with nucleotides for this to occur. Tetramers form to some extent even in the absence of nucleotides or in the presence of only s-site effectors, but the tetramers formed in the presence of dATP are more stable and probably represent a tighter structure. The tetramers induced by other effectors than dATP are destabilized by Mg^{2+}, and the dimers could, therefore, be even more predominating under enzyme assay conditions (30 mM Mg^{2+}) than in the GEMMA experiments, which are limited to Mg^{2+} concentrations $\leq$1 mM. It can therefore be concluded that tight α_4 tetramers are inactive and that the $\alpha_2\beta_2$ complex is the major active form, whereas it is less clear whether the looser α_4 tetramers have any enzymatic activity or not.

Perhaps the most striking feature discovered in the *P. aeruginosa* RNR is that the enzyme could bind two dATP molecules in the a-sites and that it lost the ability to bind both of them if the first ATP cone was removed. Because HMMER scores and amino acid comparisons supported the interpretation that only the first ATP cone is functional, this seems to be the first example of an ATP cone that can bind more than one dATP molecule. Interestingly, dATP binds to the s-site and a-sites with similar K_D values and yet it is known from before (14) that low concentrations of dATP activate CDP reduction (K_L = 3.2 μM), whereas higher concentrations were needed to inhibit it (K_L = 17 μM), just like in the enzymes that have an affinity difference between the sites. However, it should be remembered that K_D

and K_L values are not entirely equivalent because the latter is measured in the presence of substrate and is also influenced by the efficiency of oligomer formation, which occurs on a slower time scale than the rapid exchange of nucleotides in the allosteric sites. In addition, higher dATP occupancy might be needed to cause inhibition in the case of *P. aeruginosa* because there are three allosteric sites that need to be filled.

Another unique feature found in the *P. aeruginosa* enzyme is that the ATP seems to only have a passive role in the overall activity regulation. This conclusion is based on the observation that the addition of this nucleotide did not result in any change in overall activity under conditions when it was only allowed to bind to the a-site (when the s-site was saturated by dTTP). In contrast, the mouse enzyme was strongly activated by a-site ATP under these conditions (Fig. 7*C*), which stimulates the formation of $\alpha_6\beta_2$ complexes (8). The corresponding *E. coli* enzyme is instead inhibited by combinations of ATP and dGTP/dTTP (7). The only effect of a-site ATP in the *P. aeruginosa* enzyme was that it could prevent dATP from binding and thereby decrease enzyme inhibition. The role of ATP is thus more passive in *P. aeruginosa* RNR than in the other two enzymes because it only requires that ATP binds and not that it mediates any effect on its own.

The *P. aeruginosa* class I RNR is interesting from a drug development viewpoint, as demonstrated in a previous study (35). Some clinically used drugs that target the allosteric and catalytic sites of RNR, such as clofarabine and gemcitabine, have direct effects on oligomerization as well as the affinity between α and β subunits in different RNRs (12, 36, 37). The allosteric a-site of the *P. aeruginosa* enzyme seems to have a broader specificity than most other members of class I RNRs. Not only can dATP inhibit the enzyme, but so can high concentrations of dGTP (in the mM range), indicating that the site is more flexible than in other RNRs studied to date. This could be an advantage for the development of nucleotide analogs that specifically bind the a-site and inhibit the *P. aeruginosa* enzyme. The broader specificity, and perhaps also the differences in mechanism between the *P. aeruginosa* and eukaryotic RNRs, suggests that activity regulation could be a target for inhibition of DNA precursor synthesis in *P. aeruginosa*.

References

1. Hofer, A., Crona, M., Logan, D. T., and Sjöberg, B.-M. (2012) DNA building blocks: keeping control of manufacture. *Crit. Rev. Biochem. Mol. Biol.* **47,** 50–63
2. Lundin, D., Berggren, G., Logan, D. T., and Sjöberg, B.-M. (2015) The origin and evolution of ribonucleotide reduction. *Life* **5,** 604–636
3. Nordlund, P., and Reichard, P. (2006) Ribonucleotide reductases. *Annu. Rev. Biochem.* **75,** 681–706
4. Mathews, C. K. (2006) DNA precursor metabolism and genomic stability. *FASEB J.* **20,** 1300–1314
5. Aravind, L., Wolf, Y. I., and Koonin, E. V. (2000) The ATP-cone: an evolutionarily mobile, ATP-binding regulatory domain. *J. Mol. Microbiol. Biotechnol.* **2,** 191–194
6. Brown, N. C., and Reichard, P. (1969) Ribonucleoside diphosphate reductase: formation of active and inactive complexes of proteins B1 and B2. *J. Mol. Biol.* **46,** 25–38
7. Rofougaran, R., Crona, M., Vodnala, M., Sjöberg, B.-M., and Hofer, A. (2008) Oligomerization status directs overall activity regulation of the *Escherichia coli* class Ia ribonucleotide reductase. *J. Biol. Chem.* **283,** 35310–35318
8. Rofougaran, R., Vodnala, M., and Hofer, A. (2006) Enzymatically active mammalian ribonucleotide reductase exists primarily as an $\alpha_6\beta_2$ octamer. *J. Biol. Chem.* **281,** 27705–27711
9. Fairman, J. W., Wijerathna, S. R., Ahmad, M. F., Xu, H., Nakano, R., Jha, S., Prendergast, J., Welin, R. M., Flodin, S., Roos, A., Nordlund, P., Li, Z., Walz, T., and Dealwis, C. G. (2011) Structural basis for allosteric regulation of human ribonucleotide reductase by nucleotide-induced oligomerization. *Nat. Struct. Mol. Biol.* **18,** 316–322
10. Crona, M., Avesson, L., Sahlin, M., Lundin, D., Hinas, A., Klose, R., Söderbom, F., and Sjöberg, B.-M. (2013) A rare combination of ribonucleotide reductases in the social amoeba Dictyostelium discoideum. *J. Biol. Chem.* **288,** 8198–8208
11. Kashlan, O. B., Scott, C. P., Lear, J. D., and Cooperman, B. S. (2002) A comprehensive model for the allosteric regulation of mammalian ribonucleotide reductase. Functional consequences of ATP- and dATP-induced oligomerization of the large subunit. *Biochemistry* **41,** 462–474
12. Wang, J., Lohman, G. J., and Stubbe, J. (2009) Mechanism of inactivation of human ribonucleotide reductase with p53R2 by gemcitabine 5′-diphosphate. *Biochemistry* **48,** 11612–11621
13. Ando, N., Brignole, E. J., Zimanyi, C. M., Funk, M. A., Yokoyama, K., Asturias, F. J., Stubbe, J., and Drennan, C. L. (2011) Structural interconversions modulate activity of *Escherichia coli* ribonucleotide reductase. *Proc. Natl. Acad. Sci. U.S.A.* **108,** 21046–21051
14. Torrents, E., Westman, M., Sahlin, M., and Sjöberg, B.-M. (2006) Ribonucleotide reductase modularity: atypical duplication of the ATP-cone domain in *Pseudomonas aeruginosa*. *J. Biol. Chem.* **281,** 25287–25296
15. Ormö, M., and Sjöberg, B.-M. (1990) An ultrafiltration assay for nucleotide binding to ribonucleotide reductase. *Anal. Biochem.* **189,** 138–141
16. Roshick, C., Iliffe-Lee, E. R., and McClarty, G. (2000) Cloning and characterization of ribonucleotide reductase from Chlamydia trachomatis. *J. Biol. Chem.* **275,** 38111–38119
17. Reichard, P., Eliasson, R., Ingemarson, R., and Thelander, L. (2000) Cross-talk between the allosteric effector-binding sites in mouse ribonucleotide reductase. *J. Biol. Chem.* **275,** 33021–33026
18. Eriksson, S., Thelander, L., and Akerman, M. (1979) Allosteric regulation of calf thymus ribonucleoside diphosphate reductase. *Biochemistry* **18,** 2948–2952
19. Thelander, L., Eriksson, S., and Akerman, M. (1980) Ribonucleotide reductase from calf thymus: separation of the enzyme into two nonidentical subunits, proteins M1 and M2. *J. Biol. Chem.* **255,** 7426–7432
20. Eriksson, S., Gudas, L. J., Ullman, B., Clift, S. M., and Martin, D. W., Jr. (1981) DeoxyATP-resistant ribonucleotide reductase of mutant mouse lymphoma cells: evidence for heterozygosity for the protein M1 subunits. *J. Biol. Chem.* **256,** 10184–10188
21. Domkin, V., Thelander, L., and Chabes, A. (2002) Yeast DNA damage-inducible Rnr3 has a very low catalytic activity strongly stimulated after the formation of a cross-talking Rnr1/Rnr3 complex. *J. Biol. Chem.* **277,** 18574–18578
22. Hofer, A., Ekanem, J. T., and Thelander, L. (1998) Allosteric regulation of *Trypanosoma brucei* ribonucleotide reductase studied *in vitro* and *in vivo*. *J. Biol. Chem.* **273,** 34098–34104
23. Hofer, A., Schmidt, P. P., Gräslund, A., and Thelander, L. (1997) Cloning and characterization of the R1 and R2 subunits of ribonucleotide reductase from *Trypanosoma brucei*. *Proc. Natl. Acad. Sci. U.S.A.* **94,** 6959–6964
24. Hendricks, S. P., and Mathews, C. K. (1998) Allosteric regulation of vaccinia virus ribonucleotide reductase, analyzed by simultaneous monitoring of its four activities. *J. Biol. Chem.* **273,** 29512–29518
25. Berglund, O. (1972) Ribonucleoside diphosphate reductase induced by bacteriophage T4: II. allosteric regulation of substrate sepecificity and catalytic activity. *J. Biol. Chem.* **247,** 7276–7281
26. Berglund, O., and Eckstein, F. (1972) Synthesis of ATP- and dATP-substituted Sepharoses and their application in the purification of phage-T4-induced ribonucleotide reductase. *Eur. J. Biochem.* **28,** 492–496
27. Hendricks, S. P., and Mathews, C. K. (1997) Regulation of T4 phage aerobic ribonucleotide reductase: simultaneous assay of the four activities. *J. Biol. Chem.* **272,** 2861–2865
28. Brown, N. C., and Reichard, P. (1969) Role of effector binding in allosteric

control of ribonucleoside diphosphate reductase. *J. Mol. Biol.* **46,** 39–55
29. Riera, J., Robb, F. T., Weiss, R., and Fontecave, M. (1997) Ribonucleotide reductase in the archaeon *Pyrococcus furiosus*: a critical enzyme in the evolution of DNA genomes? *Proc. Natl. Acad. Sci. U.S.A.* **94,** 475–478
30. Eliasson, R., Pontis, E., Jordan, A., and Reichard, P. (1999) Allosteric control of three B12-dependent (class II) ribonucleotide reductases: implications for the evolution of ribonucleotide reduction. *J. Biol. Chem.* **274,** 7182–7189
31. Eliasson, R., Pontis, E., Sun, X., and Reichard, P. (1994) Allosteric control of the substrate specificity of the anaerobic ribonucleotide reductase from *Escherichia coli*. *J. Biol. Chem.* **269,** 26052–26057
32. Torrents, E., Buist, G., Liu, A., Eliasson, R., Kok, J., Gibert, I., Gräslund, A., and Reichard, P. (2000) The anaerobic (class III) ribonucleotide reductase from *Lactococcus lactis*: catalytic properties and allosteric regulation of the pure enzyme system. *J. Biol. Chem.* **275,** 2463–2471
33. Averett, D. R., Lubbers, C., Elion, G. B., and Spector, T. (1983) Ribonucleotide reductase induced by herpes simplex type 1 virus: characterization of a distinct enzyme. *J. Biol. Chem.* **258,** 9831–9838
34. Lundin, D., Gribaldo, S., Torrents, E., Sjöberg, B.-M., and Poole, A. M. (2010) Ribonucleotide reduction: horizontal transfer of a required function spans all three domains. *BMC Evol. Biol.* **10,** 383
35. Tholander, F., and Sjöberg, B.-M. (2012) Discovery of antimicrobial ribonucleotide reductase inhibitors by screening in microwell format. *Proc. Natl. Acad. Sci. U.S.A.* **109,** 9798–9803
36. Aye, Y., and Stubbe, J. (2011) Clofarabine 5′-di and -triphosphates inhibit human ribonucleotide reductase by altering the quaternary structure of its large subunit. *Proc. Natl. Acad. Sci. U.S.A.* **108,** 9815–9820
37. Zimanyi, C. M., Ando, N., Brignole, E. J., Asturias, F. J., Stubbe, J., and Drennan, C. L. (2012) Tangled up in knots: structures of inactivated forms of *E. coli* class Ia ribonucleotide reductase. *Structure* **20,** 1374–1383